Simulation of Cracking near a Large Underground Cavern in a Discontinuous Rock Mass using the Expanded Distinct Element Method

Yujing JIANG[1), 2)], Bo LI[3)] and Yuji YAMASHITA[4)]

[1)] Faculty of Engineering, Nagasaki University, Nagasaki 852-8521, Japan
[2)] Research Center for Geo-Environmental Science, Dalian University, Dalian 116622, P.R.China
[3)] Graduate School of Science and Technology, Nagasaki University, Nagasaki 852-8521, Japan
[4)] Kyushu Electric Power Co., Inc., Fukuoka 815-8521, Japan

Corresponding author:

Yujing JIANG, Faculty of Engineering, Nagasaki University, Nagasaki 852-8521, Japan
Tel: +81-95-819-2612
Fax: +81-95-819-2627
Email address: jiang@civil.nagasaki-u.ac.jp

for submission to - *International Journal of Rock Mechanics and Mining Science*

ABSTRACT: The rock masses in a construction site of underground cavern are generally not continuum due to the presence of discontinuities, such as bedding, joints, faults and fractures. The performance of an underground cavern is principally ruled by the mechanical behaviors of the discontinuities in the vicinity of the cavern. A number of experimental and numerical investigations have demonstrated the significant influences of discontinuities on the mechanical, thermal and hydraulic behaviors of discontinuous rock masses, indicating that the deformation mechanism and stability of rock structures in the discontinuous rock masses depend not only on the existing discontinuities but also the new cracks generated and thereafter keep propagating due mainly to the stress redistribution induced by excavation.

In this study, an Expanded Distinct Element Method (EDEM) was developed for simulating the crack generation and propagation due to the shear and tension failures in the matrix rock blocks. Using this method, excavation simulations of deep underground caverns have been carried out on the models with differing depths of cavern and differing geometrical distributions of the existing discontinuities. Model experiments by using the base friction test apparatus were conducted to verify the proposed numerical approach. Furthermore, the support effects of rock bolts on controlling the deformations of the rock mass surrounding a cavern and movements of key blocks were evaluated by means of the EDEM approach.

Keywords: Underground Cavern; Discontinuity; Crack Generation; Deformational Behavior; Support Design; UDEC

1 INTRODUCTION

Understanding the mechanical behaviors of discontinuous rock masses is important for the development and utilizations of deep underground engineering such as radioactive waste disposal facilities, power plants and petroleum reservoirs. The deformation and failure behaviors of an underground structure are principally governed by the discontinuities existing in the host rock masses. During the excavation process, the change of stress state (primary the redistribution of stresses) in the rock masses may trigger the crack generation, which combining with the pre-existing discontinuities could remarkably reduce the strengths of rock masses, endangering the stability of underground structures. To effectively assess the stability of underground structures, thorough understanding of the mechanical behaviors of existing discontinuities as well as the mechanism for crack generation and propagation is required.

The discrete element method (DEM) represents the rock mass as an assemblage of discrete blocks and the discontinuities as interfaces between blocks. It could realistically model the mechanical behaviors (compression, slip, separation) and geometrical properties (orientation, gap, spacing etc.) of discontinuities according to site investigation and therefore attracts more and more attention when studying the problems in discontinuous rock masses. A number of parametric studies have been carried out by using the DEM to estimate the behavior of rock masses with or without cavern, with one set or more than one set discontinuities [1-12]. The DEM has also been used to analyze real construction sites containing underground structures and the analytical results have been compared with the measured performance [13, 14]. These studies demonstrated the significant influences of the properties like density, dip angle, position of discontinuities on the mechanical behavior of the object underground structures and proved the effectiveness of DEM to study the underground problems in discontinuous rock masses.

In this study, an Expanded Distinct Element Method (EDEM) [15] was developed for simulating the crack generation and propagation due to the shear and tension failures in the matrix blocks based on the distinct element code UDEC [16]. Using this method, excavation simulations of a deep underground cavern have been carried out on a series of models with differing depths and differing geometrical distributions of existing discontinuities. Scale model experiments by using the base friction test apparatus were conducted on these models to verify the proposed numerical approach. Finally, the support effects of rock bolts on controlling the deformations of the rock masses surrounding the cavern and the movements of key blocks were evaluated in the numerical analyses.

2 MODELLING CRACKING RPOCESS IN ROCK MASSES

2.1 Basic numerical approach of representing crack generation in rock matrix

There have been a number of studies focusing on the cracking processes around tunnel or opening in rock masses, such as [17-21]. When an underground cavern is excavated in crystalline rock masses, crack initiation and propagation may arise by two mechanisms: (1) stress-induced cracking (short term) and (2) time-dependent cracking (long term) [21]. The first one happens principally due to the stress redistribution during the excavation process in the vicinity of cavern and it generates the main amount of new cracks comparing to the second mechanism inducing creeping damage. There are generally three numerical approaches to taking the influences of cracking into account in assessing the performance of an underground structure: (1) approach using fracture mechanics; (2) approach by transforming the mean behaviors of cracks to a continuum; (3) approach using microcracking models to evaluate the behaviors of individual cracks.

Instead of using the strength criterion, the first approach adopts the energy criterion based on the fracture mechanics in the continuum model to judge the crack generation. It is effective to represent the direction and quantity of cracking, whereas the performance changes of the structure induced by crack generation is difficult to be well assessed. The second approach is generally used in the model filled with smeared (nonpersistent) cracks, where the behaviors of individual cracks are difficult to be assessed and the influences of cracks are represented by decreasing the material properties of the continuum model. This method is effective for the total behavior assessment of a rock structure especially the ones without major persistent discontinuities.

The microcracking models representing the initiation and propagation of individual cracks provide a better solution to understand the influences of the newly generated cracks on the local performance of a rock structure. This approach treats the cracks in a model as discrete elements to facilitate the behavior assessment of every single cracks. The crack generation simulation can be accomplished by: (1) continuously rebuilding the meshes in the model according to the propagation direction of new cracks during the simulation as shown in Figure 1 [22]; (2) Pre-distributing potential cracks with bonding strengths equivalent to the rock matrix into the model and separating them when the generation criterions are satisfied. Comparing to the first method, the shortcoming of the second one is that the new cracks can only be generated on the paths of potential cracks thus the generation direction of cracks cannot be realistically predicted. When using a DEM program such as UDEC to simulate the crack generation, however, the rebuilding of meshes (zones in UDEC) during the simulation is a tough task and a time-consuming problem. To overcome the shortcoming of the second method, the propagation paths of cracking in terms of potential cracks need to be carefully

arranged in the model before simulation to provide the effective possible paths for the cracking process. In this study, the EDEM by combining the second method to UDEC was developed to accomplish the crack generation simulation in the rock masses containing a cavern as described below.

2.2 Definition of potential cracks in rock matrix

Special treatment in terms of defining the potential cracks, which could change to real cracks when satisfying the failure criterions, was applied to the DEM model to accomplish the function of crack generation. Cracks could theoretically be generated anywhere in a model, which requires potential cracks being filled with the whole model. By doing so, however, the calculation in EDEM will be extremely time-consuming and in most cases, only a few parts of potential cracks could exceed the failure criterions thus change to cracks. In this study, a prior elastoplastic analysis was carried out on the model without potential cracks to obtain the directions of principal stresses and the extent of plastic zones. The potential cracks were then distributed into the plastic zones based on the fact that new cracks are generally generated within the plastic zones. In this method, cracks can only propagate with pre-determined paths, therefore the orientation of potential cracks is an important factor for performing an accurate simulation in terms of deciding the cracking direction. The new cracks have the potential to be generated in any directions in a rock block undergoing stresses on boundaries. The numerical model, however, could not afford such large amount of potential cracks in various directions limited by the computation time. In this study, a number of regions in which the principal stresses have the same direction have been identified based on the results of prior analysis. In these regions, when shear was considered to be the principal reason to generate new cracks (i.e. shear failure region), two directions $45^\circ + \phi/2$ starting from the major principal stress plane on two opposite sides were applied to the potential cracks. When tension was considered to be the principal reason (i.e. tension failure region), then the directions parallel and vertical to the principal stress plane were applied. By doing so, two sets of potential cracks having the directions with the highest possibility for crack generation were applied in each region. In practice, the rock blocks near the sidewalls of cavern have the potential to slip or fall into the cavern, which could be generally categorized as shear failure region. The falling of blocks on the arch largely endangers the stability of cavern and they could be defined as tension failure region. The spacing of potential cracks (density) applied in the model need to synthetically consider the size of cavern and the density of the existing discontinuities as well as the computation time in EDEM. The prototype of the model in this study is an underground cavern located in Miyazaki Prefecture, Japan. According to the investigation data (cracking spacing) of this construction site and to realistically represent the generation and propagation process of cracks in the present model, 1/10 of the height of

cavern was chosen to the spacing of the potential cracks. This spacing needs modification when dealing with different problems using EDEM. A number of simulations by comparing the mechanical behaviors of the models with and without the potential cracks were carried out, with differing mechanical properties of potential cracks. By doing so, the mechanical properties of potential cracks have been carefully chosen to ensure the models with the potential cracks perform almost the same deformational behavior with the ones without potential cracks.

2.3 Failure criterions for the potential cracks

Two failure criterions are adopted according to the principal stresses acting on each potential crack to define the failure modes. Criterions for shear failure f_s and tension failure f_t can be expressed as equations (1) and (2), respectively.

$$f_s = (1.0 - \sin\phi)\sigma_1 - (1.0 + \sin\phi)\sigma_3 - 2.0c\cos\phi \tag{1}$$

$$f_t = \sigma_t - \sigma_3 \tag{2}$$

where c is the cohesion, ϕ is the friction angle of intact rock. σ_t is the tension strength of intact rock. Herein, σ_1 is major, σ_3 is minor principal stresses and compressive stresses are negative.

As shown in Figure 2, 2 groups of stress tensors (σ_{ix}, τ_{ixy}, σ_{iy})(i=1,2,3,4) locating at the two sides of a potential crack respectively are picked out. These stress tensors come from the zones (basic elements in UDEC) surrounding the calculation point on a potential crack. Principle stresses on a potential crack can be evaluated by using the Airy stress function (3), and components of stress are given by equations (4)-(6). Coefficients a, b, c and d in equation (3) are defined according to stress continuum around the calculation point.

$$\Phi = \frac{\mathrm{a}}{6}X^3 + \frac{b}{2}X^2Y + \frac{c}{2}XY^2 + \frac{d}{6}Y^3 \tag{3}$$

$$\sigma_x = \frac{\partial^2\Phi}{\partial x^2} \tag{4}$$

$$\tau_{xy} = -\frac{\partial^2\Phi}{\partial x\partial y} \tag{5}$$

$$\sigma_y = \frac{\partial^2\Phi}{\partial y^2} \tag{6}$$

The mechanical properties of the potential cracks satisfying either one of the failure criterions are reduced to that of the existing joints automatically during simulation so that new cracks could perform the same mechanical behaviors with the existing joints.

2.4 Judgment procedure of the crack generation

The judgment of crack generation and propagation in the EDEM can be carried out at each calculation step or every *n* steps depending on the limitation of computation time and the required representing accuracy of the generation process. Each potential crack could be divided into several sections by zones and the judgment is executed section by section. The number of sections for one potential crack depends on the number of zones generated around this crack. By doing so, one potential crack can totally change to new cracks in one time step (when the whole potential crack satisfies the criterions in one step) or several time steps (when only a few sections of the potential crack satisfy the criterions in one step). The judgment is executed only for the pre-defined potential cracks and ends when all of the potential cracks have been evaluated. The process of judgment mainly comprises the following three steps: (a) defining the potential cracks in the essential blocks according to the distribution features of principal stresses and plastic zones in jointed rock masses obtained from the prior analyses; (b) estimating the stress tensors around the calculation points on each potential crack and judging the propagation direction (two directions in general) and magnitude (number of sections) of new cracks by employing the shear and tension failure criterions; (c) updating the mechanical properties of the newly generated cracks.

3 EXPERIMENTAL VERIFICATION OF THE EDEM BY MEANS OF BASE FRICTION TEST

In this study, a number of base friction models were used to experimentally investigate the deformation and local failure behaviors of the underground cavern excavated in the jointed rock masses and to verify the proposed EDEM approach. In general, the base friction technique is used to demonstrate various mechanisms of failures in rocks and it has been considered as one of the most effective experimental methods to reproduce the effects of gravity in two-dimensional physical models [23]. In this study, the base friction experiments were carried out on the apparatus developed in [24], which, by assembling an image analyzing system employing a CCD camera and picture analyzing software, can directly obtain the details of deformation and cracking process in the rock mass models.

3.1 Experimental and analytical model of underground cavern

The powerhouse of an underground power plant was used as the prototype of the object deep underground cavern as shown in Figure 3. The powerhouse has a warhead sectional profile and is 48m in height and 24m in width. The depth of the cavern from the ground surface is 158m. The rock masses in the ground are fresh and hard sandstones and a region with a dimension of 200m×180m was chosen to build the experimental and numerical models. The coefficient of lateral pressure K_0=0.6 was evaluated from *in-situ* investigation, then the initial *in-situ* stresses on the boundaries of the modelling region were reproduced and the excavation simulation of the cavern without support was carried out. Full-scale model to the underground cavern was used in simulations and the model in the experiments used the geometrical scale Λ=1/400 to the prototype. The stress scale Σ was thereafter evaluated as17.86 according to the similarity law (see Figure 3) [12].

3.2 Mechanical properties of the intact rock and joints

With regard to the needs of adequately representing the behaviors of rock joints in the experimental model, a number of fundamental tests on the mechanical properties of artificial rock blocks by changing the weight ratio combination of several element materials were carried out. As a result, the artificial rock blocks were manufactured with a mixture of plaster, lime, sand and water, with weight ratio of 1:3:12:3.61. The mixture was poured into several molds and desiccated at ordinary temperature for one day and at 100 ℃ for two days in a desiccator. Three types of molds were used to manufacture the required artificial rock blocks with widths of 2cm, 3cm, and 4cm, respectively. The jointed rock masses were then formed by setting the artificial block members on the base plate with a total dimension of 45cm*50cm.

The mechanical properties of the artificial rock blocks were assessed by carrying out the unconfined compression tests and the triaxial compression tests. The triaxial compression tests were conducted in three lateral pressures of 0.1MPa, 0.15MPa and 0.2MPa, by applying the Mohr's stress circle on the results of which, the cohesion and friction angle were acquired with values c=0.143MPa and ϕ=34° , respectively. Other properties of the artificial rock blocks are: unconfined compressive strength σ_c=0.92MPa, density ρ=1.505 g/cm^3, Young's modulus E=415.52 MPa, Poisson's ratio ν=0.136 and tension strength σ_t=0.0546 MPa.

To facilitate crack generation, the artificial rock blocks used in this study are very brittle with low strength, consequently it is difficult to use conventional shear test apparatus to evaluate their shear behaviors. In this study, an improved shear test apparatus was adopted in shear tests [12]. This test apparatus has a special designed shear box unit, in which the lower part is larger than the upper part throughout the full shear process, so as to keep a constant

contact area of specimens in the shear process. The delicate loading units afford the shear tests in very low stress conditions on which the shear behaviors of specimens could also be accurately measured. Direct shear tests with three patterns of normal stresses 0.1MPa, 0.15MPa and 0.2MPa were applied on the artificial rock blocks to acquire the necessary mechanical properties for numerical analyses. The shear test results are demonstrated in Figure 4 and Figure 5. The normal loading tests have been carried out on the artificial rock blocks with and without fracture to acquire the total normal displacement u_{totoal} and intact normal displacement u_{intact}, respectively. Then, the normal behavior of the joint can be derived from $u_{joint} = u_{totoal} - u_{intact}$. The normal stress-normal displacement relationship shows nonlinearity in Figure 5, which can be divided into 3 sections (Ⅰ, Ⅱ, Ⅲ) and their normal stiffness are $K_{n\,Ⅰ}$=260.0MPa/m, $K_{n\,Ⅱ}$=940.0MPa/m, $K_{n\,Ⅲ}$=1880.0MPa/m, respectively. A regression function (7) was then deduced based on the curve in Figure 5 to predict the experimental results beyond these three sections as follows.

$$\sigma_n = -4.302v^3 + 7.688v^2 - 0.123v \qquad R^2=0.9987 \tag{7}$$

where v is normal displacement, σ_n is normal stress and R is residual. Other properties of the rock joints are: shear stiffness K_s =80.7MPa/m, cohesion c_j =0MPa, friction angle ϕ_j =31.2° and tension strength σ_{tj} = 0MPa. It should be noted that the artificial rock blocks have been polished before tests and their surfaces are very flat and smooth. Therefore, the contacts among them have non-cohesion and non tensile strength. After being polished, all of the blocks in a model have alike surface conditions, so that universal joint properties can be applied to them in simulations. The necessary mechanical properties for numerical analyses were calculated from the experimental results of artificial rock blocks by using the similarity law.

3.3 Distribution characteristics of rock joints in experiment and numerical analyses

The distribution characteristic of rock joints including the dip angle, spacing, gap etc. in rock masses is one of the key factors that influence the deformational behaviors of underground caverns. To acquire a rational understanding, more than 10 patterns of joint distributions have been investigated by changing the dip angle and spacing of joints in both experiments and numerical analyses, among which, 3 patterns are compared and demonstrated at here as shown in Table 1. In the table, α is the dip angle and d is the spacing between two joints converted from the dimensions of experimental models by using the similarity law. The cuboid artificial rock blocks were firstly set on the plate of the base friction apparatus to build the jointed rock mass model. Since the model is composed of many such blocks and initially they don't contact closely with each others, stresses on the boundaries and air pressure

vertical to the model were applied with reduced values (1/5) to consolidate the model. After that, the cavern in the center of model was excavated and full-scale stresses evaluated from *in-situ* stresses by using stress scale Σ were applied to locate the model in required stress condition. Herein, the air pressure vertical to the test model is used to change the frictional forces acting on the model. In numerical analyses, before excavation, equilibrium under the gravity of rock mass in the study area and boundary conditions undergoing the stresses from the surrounding rock masses was achieved to consolidate the blocks in the model. The preparations for the crack generation have been conducted in the numerical analyses as stated in section 2.1. Noting that in both the model tests and numerical analyses, the reinforcements on the wall of cavern have not been considered due to the difficulties in reproducing the reinforcements in base friction model tests and to facilitate the crack generation.

3.4 Comparison of the experimental and analytical results

Figure 6 (a), (b) and (c) show the close-up images of the newly generated cracks marked as "×" in the vicinity of cavern in experiments for cases 1, 2, and 3, respectively. The new cracks were identified by using the image analyzing system, where only the locations of new cracks have been marked and the widths of cracks were not taken into account in this study. In Case 1, the new cracks are mainly distributed near the right sidewall of cavern concentrating in one rock block. The new cracks in Case 2 and Case 3 are distributed in more dispersed positions, most of which are also near the right sidewall. Therefore, the slide of large blocks in the right sidewall of cavern may have participated the major parts of deformation of the rock mass for all the three cases. Since the reinforcements were not conducted, the tension failure has become the principal reason to generate new cracks.

The distributions of new cracks obtained from numerical analyses give similar tendency to the images in the model experiments as demonstrated in Figure 6 (d), (e) and (f). The numerical results of Case 1 captured the assembly of cracks near the right sidewall and a few cracks on the left arch. Case 2 captured the cracks near the upper right sidewall and Case 3 captured the cracks near the upper right sidewall and the lower left sidewall. When the dip angle of joints becomes steeper, the generation positions of new cracks trend to move to the relatively upper position near the sidewall by comparing Case 2 and Case3 with Case1. Case 3, with shorter joint spacing, produced more new cracks comparing to Case 2 with the same dip angle. Most of the new cracks were generated by satisfying the judgment criterion (2) (tension failure), which agrees with the failure mode taking place in the model experiments. The generation amount of new cracks in numerical analyses are generally larger than the model tests due to (1) there are more intersecting joints (vertical to the main joint set, especially in Case (2) in numerical models than that in experiments; (2) the mechanical properties used in analyses converted from the properties of artificial rock blocks by using the

similarity law may have been slightly underestimated; (3) the CCD camera based image analyzing system cannot capture the cracks generated in the interior of the artificial rock blocks and may have failed to capture a few extremely fine cracks. Although the artificial rock blocks were carefully manufactured, the heterogeneity of materials could not be totally eliminated, which could influence the experimental performance. Nevertheless, the proposed EDEM has provided reliable predictions to the crack generation process, which could help us investigate the influences of newly generated key blocks on the stability of large-scale underground cavern.

4 SIMULATIONS OF EXCAVATION PROCESS OF LARGE-SCALE UNDERGROUND CAVERN

4.1 Excavation simulation of cavern without reinforcements

A typical excavation process of underground cavern was simulated by using the EDEM as demonstrated in Figure 7. The center part of arch was drilled at the first step and then the left and right parts of arch were excavated in the steps 2 and 3. After that, bench excavation was carried out orderly from step 4 to step 16. The aforementioned joint distribution patterns, Case 1, Case 2 and Case 3, were adopted in the simulations to investigate the behaviors of key blocks produced by the new cracks that are highly unfavorite to the stability of cavern. The magnitude of stresses in the rock masses encompassing the cavern is another important factor that influences its performance. In order to take this factor into account, three different magnitudes of stresses corresponding to the depths (from the ground surface to the roof of cavern, see Figure 3) of 158m, 212m, 262m were selected. The mechanical properties of rock masses and rock joints as well as the methods for the crack generation were the same with that stated in Chapter 3.

At first, elastoplastic analyses were carried out by using UDEC to acquire the region of plastic zones and the directions of principal stresses. Figure 8 shows the plastic failure zones in jointed rock masses around the cavern in Case 3 (Depth: H = 158m) at different excavation steps ((a) after arch excavation; (b) after 9th excavation;(c) after final bench excavation). Only two small failure zones are generated near the right roof after the arch excavation. After the 9th excavation, the plastic zones spread to the two sidewalls but still in small content. As the final bench was excavated, a large connected plastic zone is generated in the rock blocks on the right sidewall, which has collapsed into the cavern, and a plastic zone in a smaller area is produced in the lower left sidewall. In the *in-situ* condition, however, before such large deformation takes place, a great number of new cracks would have been generated in the rock blocks and the movements of the newly generated key blocks could remarkably change the

failure modes of the rock masses, adequate evaluation of which requires more elaborate models capable of crack generation simulation.

Figure 9 illustrate the propagation of new cracks and the process of local failure around cavern due to excavation. The new cracks generated after arch excavation are few in Case 1 and Case 2. At the same time, Case 3 produces more new cracks along the roof wall due to the higher density of the existing joints. During the bench excavations, Case 1 and Case 2 produce almost equivalent new cracks in amount on the right side, differing in that the new cracks in Case 2 are in higher position comparing to Case 1 on the right side and are larger in amount on the left side because the existing joints in Case 2 have steeper dip angle than that of Case 1. On the other hand, because Case 3 has steeper dip angle and shorter spacing of the existing joints, the amount and area of the newly generated cracks are much larger than that in Case 1 and Case 2 when the whole excavation are finished, which lead to the separation of key blocks taking place along the new cracks on the walls of cavern. The amount and area of new cracks are furthermore increased by locating the cavern in deeper underground by comparing Figure 9 (c) (H=158m) to (d) (H=262m). For all the cases, the positions where the existing joints encountering the wall of cavern are favorable for the crack generation and propagation. The EDEM analyses provide more realistic results to the large deformation in jointed rock masses than the DEM analyses by comparing Figure 9 (c) to Figure 8 (c). The results above reveal that the local failure zones are significantly influenced by the dip angle, spacing of the existing joints and their relative position to the cavern as well as the depth of cavern.

4.2 Evaluation of the support effect of rock bolts by using EDEM

For underground structures excavated in jointed rock masses in deep underground, the most common types of failure are those involving key blocks falling from the roof or sliding out of the sidewalls of cavern. These key blocks are formed by the existing discontinuities encountering the walls of cavern as well as the newly generated cracks due to excavation. Therefore, the reinforcements need to be applied for underground structures, the design of which requires the thorough understanding of the support effects of the reinforcement components like anchor and rock bolt. Many underground structures are designed and constructed, based on the pre-investigation of the construction site and the conventional load/capacity/safety-factor approaches. To achieve more rational prediction of rock behavior and support design for deep underground cavern in jointed rock masses, analyses considering the coupled performances of rock masses and reinforcement components are required. With the development of numerical analysis approaches, effectively modelling the excavation process and the construction of supports such as grouting, rock bolt and cable has become possible in the numerical simulations.

The basic model of rock bolt in the EDEM is shown in Figure 10. The rock bolt is divided into a number of segments with nodal points located at the ends of each segment and the mass of each segment is lumped at the nodal points to facilitate the calculation. Shearing resistance is represented by spring/slider connection between a node and the rock elements encompassing the node. In this study, the reinforcement effect of rock bolts in two patterns was evaluated based on Case 3 (H=158m). The values of required input parameters for rock bolt are as follows: density 6083 kg/m^3, Young's modulus 1.9×10^5MPa, compressive yield strength 1.55MPa, tensile yield strength 1.55MPa, extensional failure strain 3.5% and cross-sectional area 446.0mm^2. The compressive strength of grouting material is 180MPa, and the shear modulus is 0.6MN.

The grouted rock bolts are embedded vertically to the walls of cavern after each excavation step. In pattern (1), the rock bolts are 5m long, and embedded in 1.5m intervals along the roof and sidewalls as shown in Figure 11 (a), (b), (c). Comparing with the no bolting pattern (see Figure 9 (c)), the bolted pattern (1) successfully inhibits the generation of key blocks on the roof and sidewalls and the total amount of new cracks is significantly decreased. The new cracks are mainly generated near the lower left sidewall (B) and the upper right sidewall (A), which could be considered as the weak zones in this model. To effectively control the deformation and crack generation in these weak zones, a further reinforced pattern (2) is evaluated as shown in Figure 11 (d), (e), (f). In pattern (2), the longer rock bolts (15m) are placed on the lower left sidewall and upper right sidewall to control the degradation of weak zones. The amount of new cracks as well as the displacements above roof (see Figure 12) have been slightly decreased in pattern (2), exhibiting good support effect comparing to the model without reinforcements. The displacements on the right side of cavern are larger than the left side in Figure 12 due to the deformation happened in the weak zones A. Although the differences between pattern (1) and pattern (2) are not obvious in the current results, considering the time-dependence of the strengths of the weak zones, the reinforcement like pattern (2) may benefit the long-term stability of the cavern in practice.

5 CONCLUSIONS

The excavation process of an underground cavern leads to the stress redistribution in the rock masses around the excavated parts, facilitating the crack generation and propagation. The newly generated cracks could significantly influence the deformational behavior of a cavern especially in terms of creating unfavorite key blocks on the roof and sidewalls. In this paper, a numerical approach, the expanded distinct element method (EDEM), is proposed to represent the generation and propagation of the new cracks in the rock masses encompassing a large-scale cavern due to excavation process. A base friction test technique and an image

analyzing system are developed, which could effectively capture the deformational behaviors as well as the presence of new cracks in the rock masses. By using these techniques, model tests of an underground cavern excavated in the deep jointed rock masses with three different distribution patterns of rock joints are conducted. Modelling of these base friction tests is also carried out in the EDEM simulations. Ideal agreements between the numerical simulations and the model tests have been identified. The support effects of rock bolts on controlling the deformation of rock masses and generation of new cracks are furthermore investigated by using the proposed numerical approaches.

The model tests and numerical simulations reveal that both the dip angle and spacing of rock joints have large influences on the amount and position of new cracks. The amount of new cracks generally increases with the increase of dip angle and decrease of joint spacing. On the dipping towards side (right side of carven in this study), the new cracks are mainly located in the upper position of sidewall since in this situation, the blocks principally exhibit slide movements towards cavern, producing the tension failure zones along the rock joints. On the dipping away side (left side of carven in this study), the new cracks mainly occur in the positions where the rock joints encountering the sidewall as well as the portion of arch a joint bypassing. The amount and area of new cracks also increase as the depth of cavern and initial ground stress increase. The support effect of rock bolts is significant in terms of largely inhibiting the deformation of rock masses and the amount of new cracks as well as controlling the generation of unfavorite key blocks on the walls. The EDEM simulations have also demonstrated the concentration of new cracks in a few weak zones, the positions of which change with the distribution patterns of the existing rock joints. Enforcements on such weak zones are required to control the crack generation and to achieve a long-term stability of a cavern.

ACKNOWLEDGEMENTS

The authors wish to thank Dr. J. Xiao, Dr. K. Nakagawa and Mr. K. Yamaguchi for their kind assistance throughout this study. This study has been partially funded by Kyushu Electric Power Co., the Ministry of Education, Japan, Grant-in-Aid for Scientific Research (B), Research Project Number 11555131 and the National Natural Science Foundation of China (No. 50028403).

REFERENCE

[1] Schwer LE, Lindberg HE. Application brief: a finite element slideline approach for calculating tunnel response in jointed rock. Int J Num Anal Methods Geomech 1992;16:529-540.
[2] Zhao J, Chen SG. A study of UDEC modelling for blast wave propagation in jointed rock masses. Int J Rock Mech Min Sci 1998;35:93-99.
[3] Cundall PA. A computer model for simulating progressive large scale movements in blocky rock system. In: Proc Symp Int Soc Rock Mech, Nancy, France, Vol. 1, 1993.
[4] Kulatilake PHSW, Ucpirti H, Wang S, Radberg G, Stephansson O. Use of the distinct element method to perform stress analysis in rock with non-persistent joints and to study the effect of joint geometry parameters on the strength and deformability of rock masses. Rock Mech Rock Engi 1992;25:253-274.
[5] Souley M, Homand F. Stability of jointed rock masses evaluated by UDEC with an extended Saeb-Amadei constitutive law. Int J Rock Mech Min Sci 1996;33:233-244.
[6] Shen B, Barton N. The disturbed zone around tunnels in jointed rock masses. Int J Rock Mech Min Sci 1997;34:117-125.
[7] Bhasin R, Hoeg K. Parametric study for a large cavern in jointed rock using a distinct element model (UDEC-BB). Int J Rock Mech Min Sci 1998;35:17-29.
[8] Suorineni FT, Tannant DD, Kaiser PK. Determination of fault-related sloughage in open stopes. Int J Rock Mech Min Sci 1999;36:891-906.
[9] Hao YH, Azzam R. The plastic zones and displacements around underground openings in rock masses containing a fault. Tunnelling Underground Space Technol 2005;20:49-61.
[10] Jiang Y, Tanabashi Y, Li B, Xiao J. Influence of geometrical distribution of rock joints on deformational behavior of underground opening. Tunnelling Underground Space Technol 2006;21:485-491.
[11] Jiang Y, Tanabashi Y, Nakagawa M. Modeling of Rock Joints and Application to Undergund Openings in Discontinuous Rock Masses by using DEM. In: Proceedings of International Conference on Geotechnical & Geological Engineering(GeoEng2000), Australia, 2000, CD-ROM, UW0711.
[12] Jiang Y, Xiao J, Yamaguchi K, Tanabashi Y, Esaki T. Mechanical behavior and support design of large underground opening in discontinuous rock masses. Journal of the Mining and Materials Processing Institute of Japan 2001;117:639-644.
[13] Bhasin RK, Barton N, Grimstad E, Chryssanthankis P, Shende FP. Comparison of predicted and measured performance of a large carvern in the Himalayas. Int J Rock Mech Min Sci 1996;33:607-626.
[14] Souley M, Homand F, Thoraval A. The effect of joint constitutive laws on the modelling

of an underground excavation and comparison with in situ measurements. Int J Rock Mech Min Sci 1997;34:97-115.
[15] Nakagawa M, Jiang Y, Esaki T. A new approach of modeling generation and progress of cracks in discontinuous rock masses by using DEM. Journal of Geotechnical Engineering, Japan Society of Civil Engineers, 1999;No.631/3-48:397-410.
[16] Itasca Consulting Group, Inc. UDEC-Universial Distinct Element Code. Version 3.0, User Manual, Minnesota, USA, 1998.
[17] Wong RHC, Lin P, Tang CA, Chau KT. Creeping damage around an opening in rock-like material containing non-persistent joints. Engineering Fracture Mechanics 2002;69:2015-27.
[18] Germanovich LN, Dyskin AV. Fracture mechanisms and instability of openings in compression. Int J Rock MechMin Sci 2000;37:263–84.
[19] Martin CD, Read RS, Martion JB. Observations of brittle failure around a circular test tunnel. Int J Rock MechMin Sci1997;34(7):1065–73.
[20] Souley M, Homand F, Pepa S, Hoxha D. Damage-induced permeability changes in granite: a case example at the URL in Canada. Int J Rock MechMin Sci 2001;38:297–310.
[21] Golshani A, Oda M, Okui Y, Takemura T, Munkhtogoo E. Numerical simulation of the excavation damaged zone around an opening in brittle rock. Int J Rock Mech Min Sci 2007;44:835-845.
[22] Nakagawa K. Numerical approaches of rock mass behaviors considering crack generation and large deformation. Ph. D thesis, Kyushu University, Fukuoka, Japan, 1999.
[23] Bray JW, Goodman RE. The Theory of Base Friction Models. Int J Rock Mech Min Sci 1981;18:453-468.
[24] Jiang Y, Esaki T. Evaluation of the behavior of underground opening using the new base friction experimental technique. Soil and Foundation, JGS 1998;46:21-24.

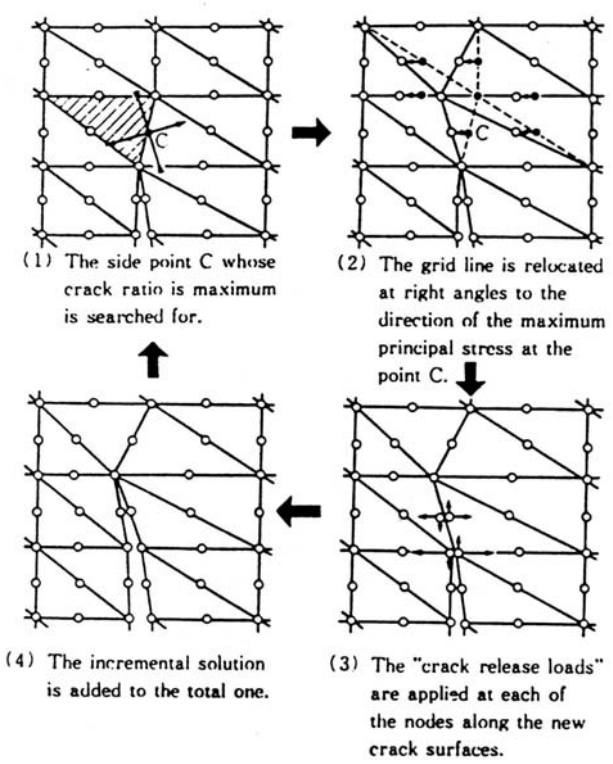

Figure 1. The method by relocating the grid lines to accomplish the crack generation.

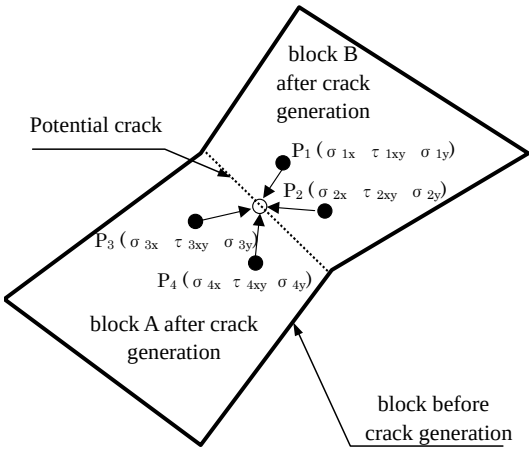

Figure 2. Definition of the principle stresses for each potential crack in EDEM model.

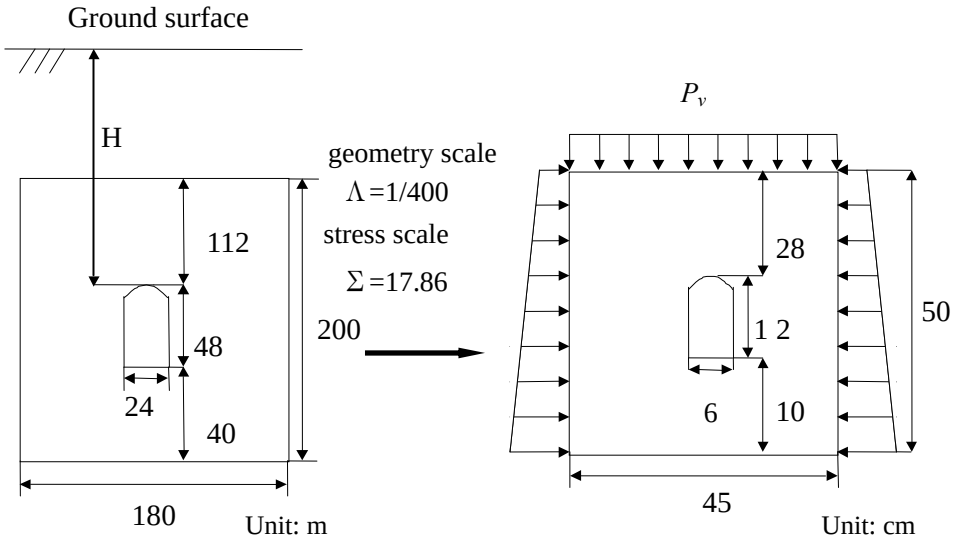

(a) prototype (b) experimental model

Figure 3. Geometrical comparison of the prototype of underground cavern in numerical analyses with the experimental model in base friction tests.

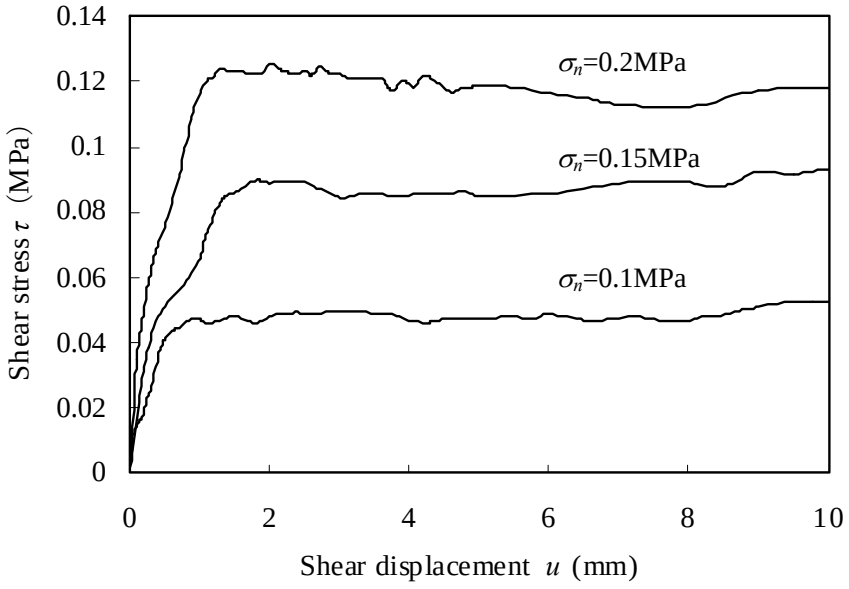

Figure 4. Shear behaviors of the artificial rock joints subjected to three kinds of normal stresses.

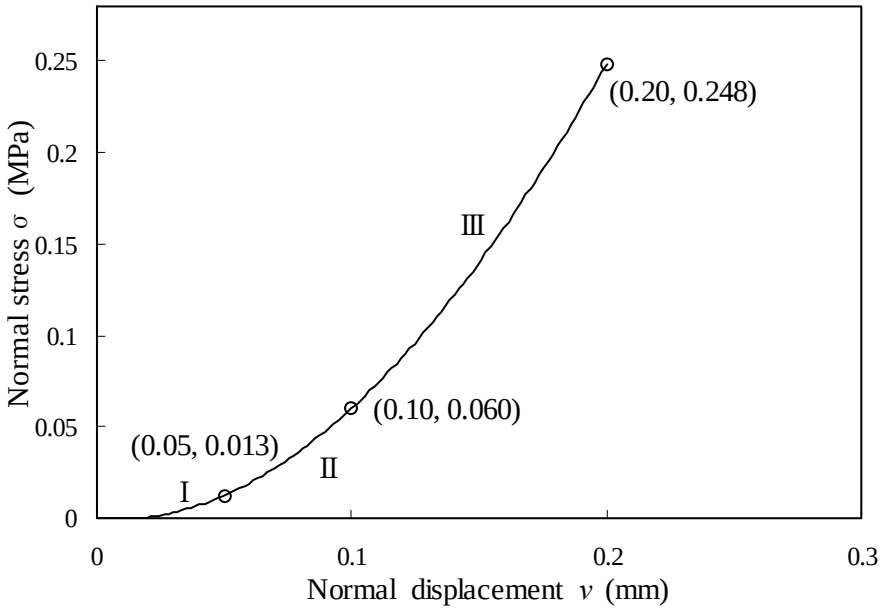

Figure 5. Deformational behavior of artificial rock joints in normal loading tests.

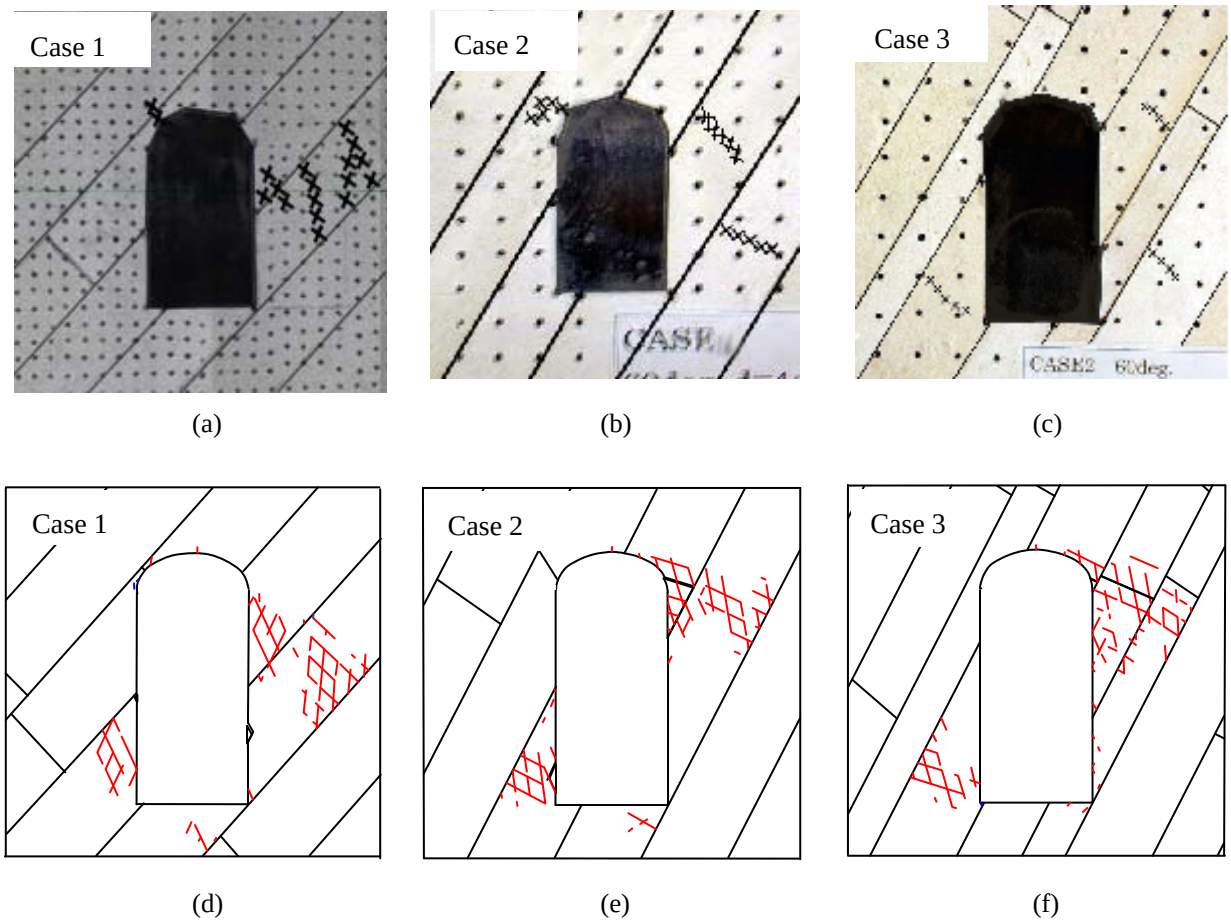

Figure 6. Comparisons of the newly generated cracks by model experiments ((a), (b), (c)) and numerical analyses ((d), (e), (f)) using the EDEM.

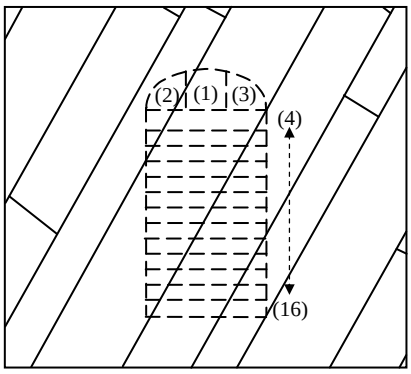

Figure 7. Numerical modelling of the excavation process.

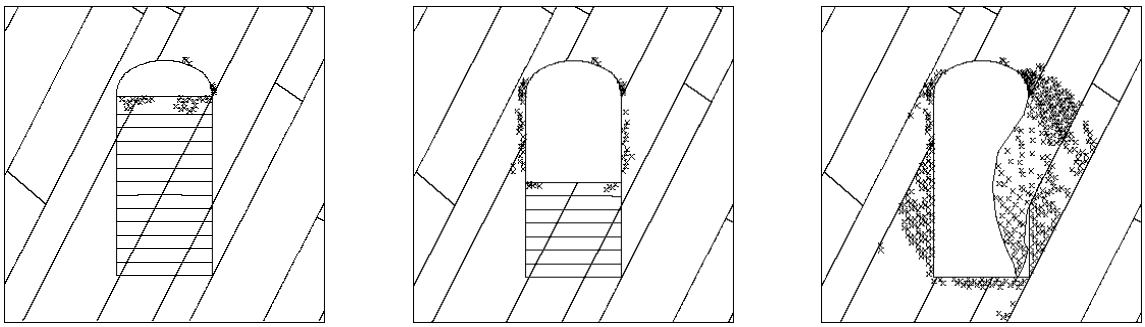

(a) (b) (c)

Figure 8. Propagation of plastic zones during excavation of Case 3. (a) after arch excavation; (b) after 9th excavation; (c) after final bench excavation.

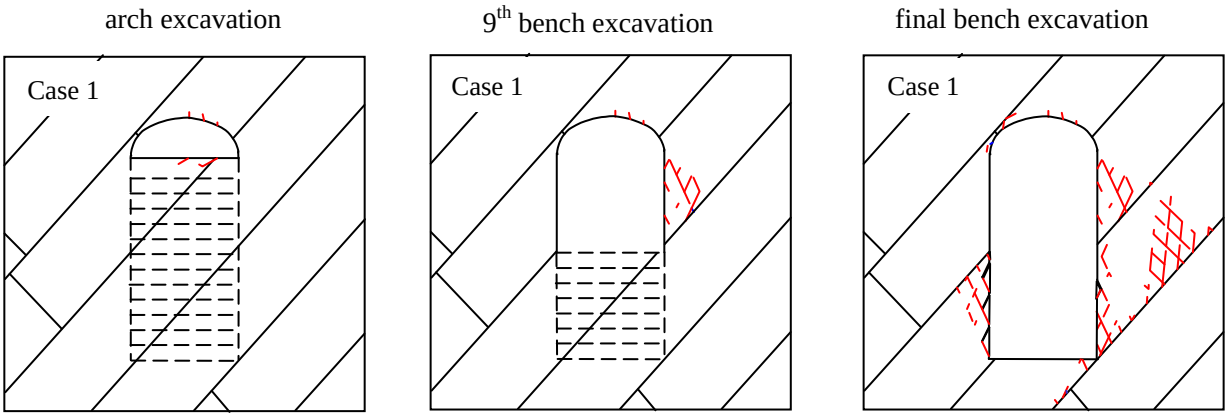

(a) Depth of underground cavern (case 1): H = 158 m

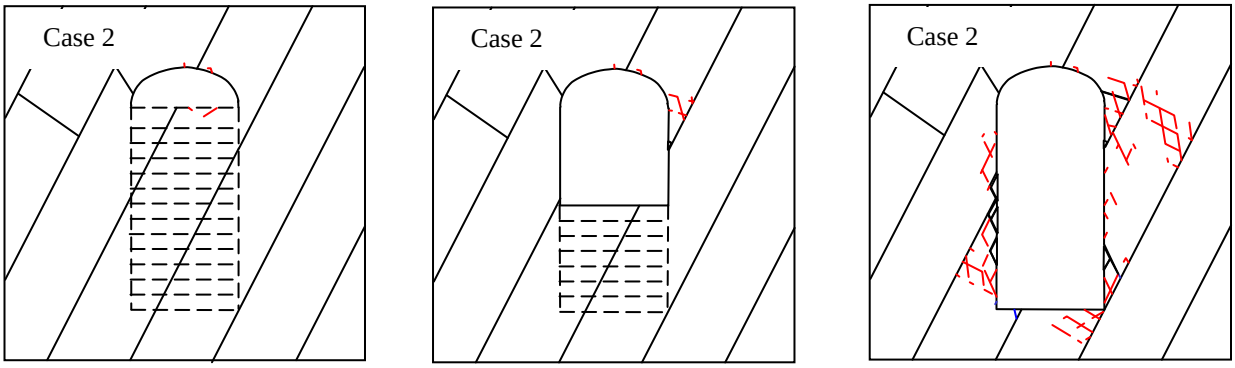

(b) Depth of underground cavern (case 2): H = 158 m

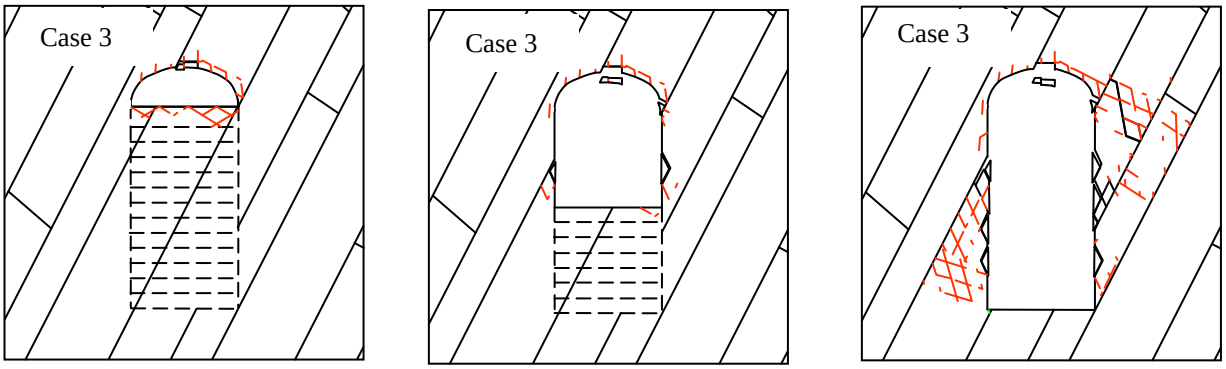

(c) Depth of underground cavern (case 3): H = 158 m

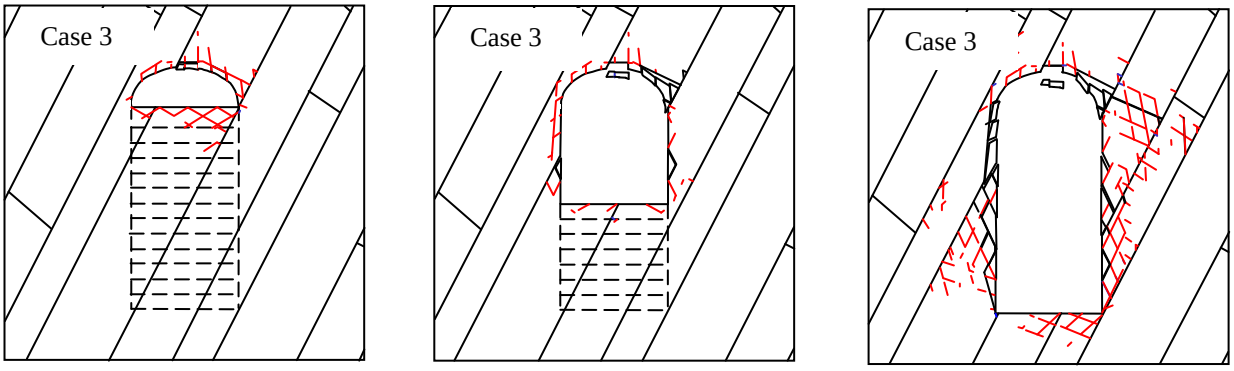

(d) Depth of underground cavern (case 3): H = 262 m

Figure 9. New crack generation during the excavation process.

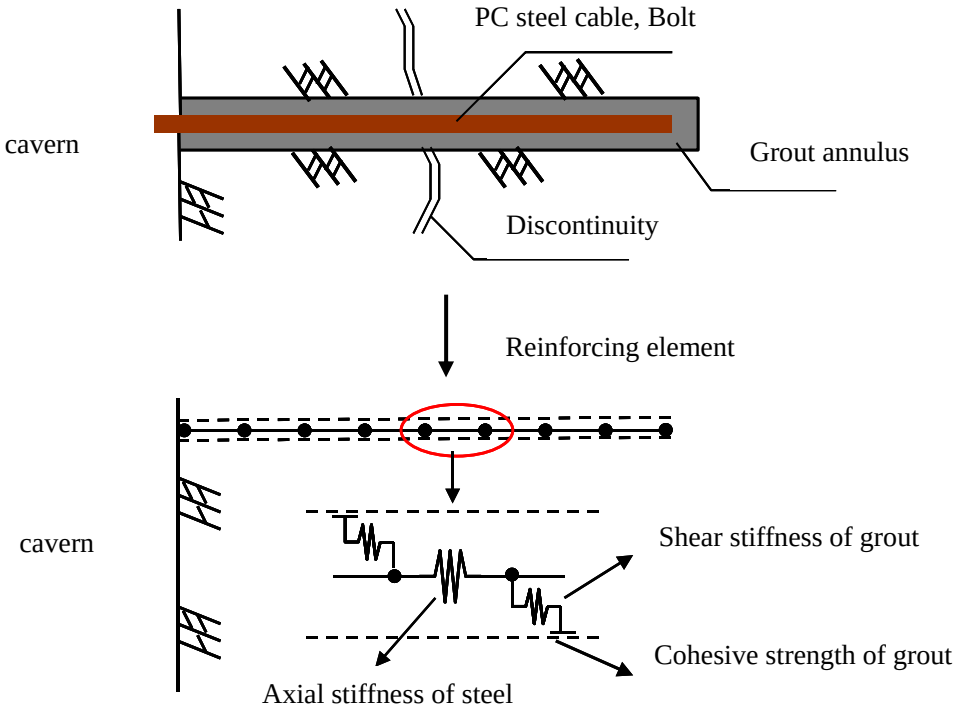

Figure 10. Illustration of the model for rock bolts in the EDEM simulation.

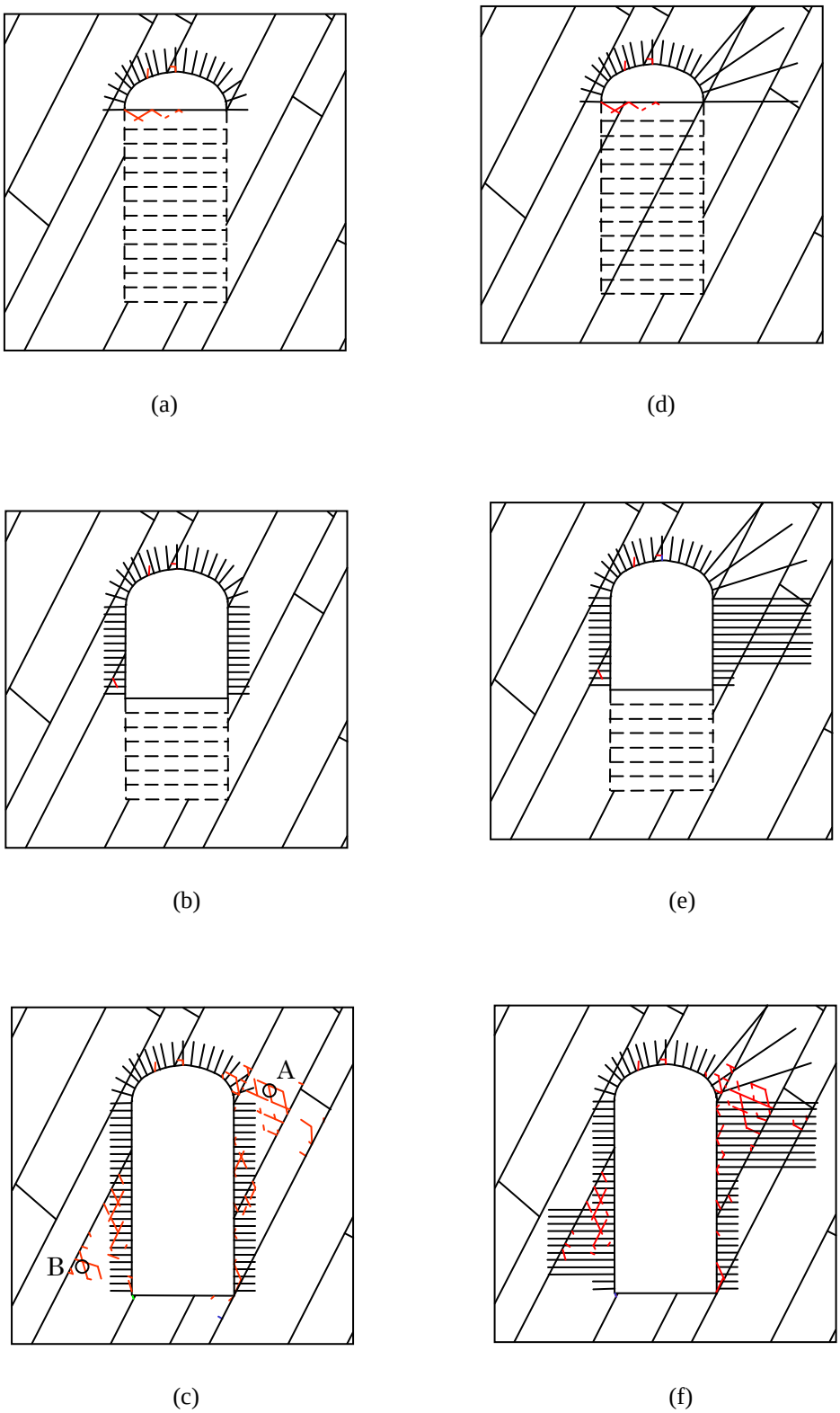

Figure 11. Illustration of the crack generation in the rock masses with two patterns of rock bolting system (pattern (1): (a), (b), (c); pattern (2): (d), (e), (f)). (A, B: weak zones)

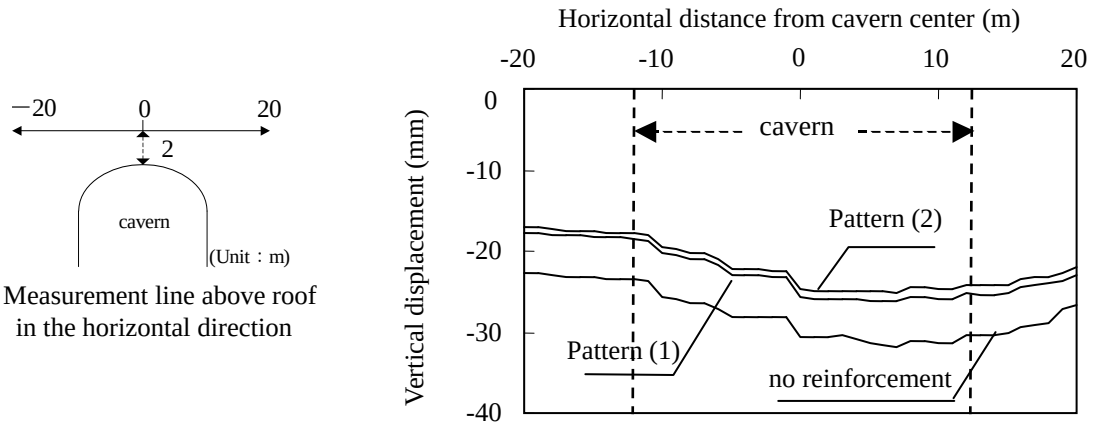

Figure 12. Comparisons of the vertical displacements along the horizontal direction above the roof of pattern (1), pattern (2) and no reinforcement pattern.

Table 1. Experimental cases.

Case	(1)	(2)	(3)
Dip angle of joint α (°)	45	60	60
Spacing of joint *d* (m)	16	16	16, 12, 8